

Metal-nanotube composites as radiation resistant materials

Rafael I. González,¹ Felipe Valencia,¹ José Mella,¹ Adri C. T. van Duin,² Kang Pyo So,³ Ju Li,³ Miguel Kiwi,^{1,a)} and Eduardo M. Bringa⁴

¹*Departamento de Física, Facultad de Ciencias, CEDENNA, Universidad de Chile, Casilla 653, Santiago 7800024, Chile*

²*Department of Mechanical and Nuclear Engineering, The Pennsylvania State University, University Park, Pennsylvania 16802, USA*

³*Department of Nuclear Science and Engineering and Department of Materials Science and Engineering, Massachusetts Institute of Technology, Cambridge, Massachusetts 02139, USA*

⁴*CONICET and Facultad de Ciencias Exactas y Naturales, Universidad Nacional de Cuyo, Mendoza 5500, Argentina*

(Received 7 March 2016; accepted 9 July 2016; published online 20 July 2016)

The improvement of radiation resistance in nanocomposite materials is investigated by means of classical reactive molecular dynamics simulations. In particular, we study the influence of carbon nanotubes (CNTs) in an Ni matrix on the trapping and possible outgassing of He. When CNTs are defect-free, He atoms diffuse alongside CNT walls and, although there is He accumulation at the metal-CNT interface, no He trespassing of the CNT wall is observed, which is consistent with the lack of permeability of a perfect graphene sheet. However, when vacancies are introduced to mimic radiation-induced defects, He atoms penetrate CNTs, which play the role of nano-chimneys, allowing He atoms to escape the damaged zone and reduce bubble formation in the matrix. Consequently, composites made of CNTs inside metals are likely to display improved radiation resistance, particularly when radiation damage is related to swelling and He-induced embrittlement. *Published by AIP Publishing.* [<http://dx.doi.org/10.1063/1.4959246>]

Nanolayered¹ and nanocrystalline materials² have attracted attention since grain boundaries act as defect sinks, while in nanofoams that role is played by the pore surfaces.³ For nuclear applications, Oxide Dispersion Strengthened (ODS) steels have been extensively studied as candidates for structural materials in the new generation of nuclear reactors. In ODS steels, the phase-boundaries between the matrix and the oxide act as defect-sinks. Carbon NanoTubes (CNTs) are slender objects that can have aspect ratios exceeding 1000, and therefore theoretically require only 0.1 vol. % (well within experimental range and economic feasibility for bulk metals) to reach the geometric percolation threshold in the case of completely random dispersion;^{4,5} some of those defects could be transported alongside the CNT axis globally, and possibly be eliminated at an outer surface.

In addition to typical radiation induced defects like interstitials and vacancies,⁶ He production in nuclear reactors⁷ can lead to He bubbles, which in turn leads to swelling⁸ and embrittlement,⁹ decreasing the lifetime of the reactor components. Metal + CNT composites might provide plenty of incoherent interfaces that could trap He. In fact, Al + CNT composites have recently been synthesized and shown, in experiments by Li and co-workers,⁴ to lead to bubble-free matrices.

In spite of the large number of studies dealing with He in metals there are still many open questions on the subject, with large discrepancies among experimental results on He diffusion in Ni.¹⁰ Bombardment of Ni with 40 keV He with fluencies of up to $5 \times 10^{20}/\text{m}^2$ leads to bubbles of a few nm in size and nearly 1% swelling.¹¹ The He bubble radius in Ni depends on temperature,¹² and for 1000 K it is ~ 1 nm. He

bubbles form preferentially at certain defective spots, such as dislocations,¹³ interfaces, and nanoparticles.¹⁴

As mentioned above, the He outgassing was already reported,^{4,5} but no specific mechanism was proposed to explain the dynamics. Here we focus our attention on the development of a detailed model for this phenomenon, which in addition is supported by molecular dynamics (MD) computations. This way, a consistent physical picture emerges, which shows that the diffusion of the He atoms occurs either along the interface between the CNTs and the Ni matrix, or by the He atoms crossing the CNT wall. Once the He penetrates into the CNT, the latter acts as a sort of chimney for the He outgassing process.

The classical reactive Molecular Dynamics (MD) simulations were performed with the Large-scale Atomic/Molecular Massively Parallel Simulator (LAMMPS) code,¹⁵ to model the influence of CNTs He trapping in an Ni matrix, and its possible outgassing capability as a 1D transport network. For the atomic interactions the ReaxFF force field¹⁶ was used, since it has proven to be adequate to model Ni-C interactions,¹⁷ the mixtures of metals with noble gases,¹⁸ and also C with noble gas atoms.¹⁹ In our simulations, we employed a recent ReaxFF implementation that combines these Ni/C/H/noble gas parametrizations. The noble gas interacts with the Ni and C-atoms only through van der Waals interactions, which are described in ReaxFF using a Morse potential. The noble gas/Ni and noble gas/C interaction parameters are derived through combination rules. In all of our calculations we use a time step of 0.5 fs and a Nosé–Hoover isenthalpic (NPH) ensemble, coupled to temperature rescaling. A 500 fs damping factor is used for the pressure control and the temperature rescaling was verified every 10 time steps, and applied

^{a)}Electronic mail: m.kiwi.t@gmail.com

only when the system deviated $\sim 5\%$ from the imposed temperature. Dynamic charge equilibration is realized at every time step. For the graphics and postprocessing of the results we use the Open Visualization Tool (OVITO) code.²⁰

We model our system as an Ni box, with sides between 2.5 and 4.5 nm, with periodic boundary conditions in all directions, and with a single embedded CNT with its axis parallel to the z -axis, and spanning the entire matrix. We have used (10,0) and (20,0) CNTs, and radiation damage was simply included as a random distribution of single vacancies, since in face-centered cubic (FCC) metals the interstitial mobility is large.¹⁰ 10% of the Ni atoms were replaced at random by He. Then this box was relaxed at 1000 K, with a barostat set at 1 atm pressure, during a few ns. After relaxation the evolution was followed during 4–5 ns at the constant pressure of 1 atm, and a constant temperature of 1000 K. We take as baseline result an Ni box, with vacancies and He, but without the CNT.

In the sample studied, strain at the CNT-metal interface is relatively low; however, large strain levels might modify the He storage capacity. Dislocations interacting with the CNTs⁵ might offer additional free volume and strain localization²¹ which might also alter He storage. We have calculated atomic strain using OVITO,²⁰ comparing the initial, unrelaxed configuration, with the relaxed high temperature configuration quenched to 1 K to remove thermal noise. This yields an upper limit to the strain in our sample. We find that only 0.6% of the Ni and C atoms display a strain larger than 5%, as expected with the Ni atoms located at the CNT interface. We do not observe any clustering of these strained atoms leading to strained volumes which might accumulate He.

Fig. 1 shows the potential energy (PE) of the He atoms, and displays a significant energy reduction for He close to the CNT, for a $3.6\text{ nm} \times 3.6\text{ nm} \times 2.1\text{ nm}$ box, with a 1 nm diameter CNT. The histogram of fraction of He atoms vs. PE shows a distinct peak, related to He clustering, in the vicinity of the CNT.

In both the pure Ni and the Ni + CNT samples, He rapidly diffuses and agglomerates into bubbles. However, as can be observed in Fig. 2, bubbles do form preferentially alongside the CNT wall. Ni atoms close to the CNT wall rapidly migrate

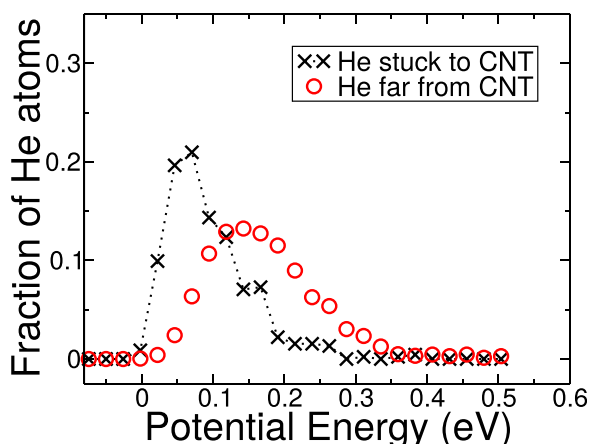


FIG. 1. Fraction of He atoms versus their potential energy. When the He bubbles stick to the CNT wall, the energy is reduced as compared with He in the Ni matrix.

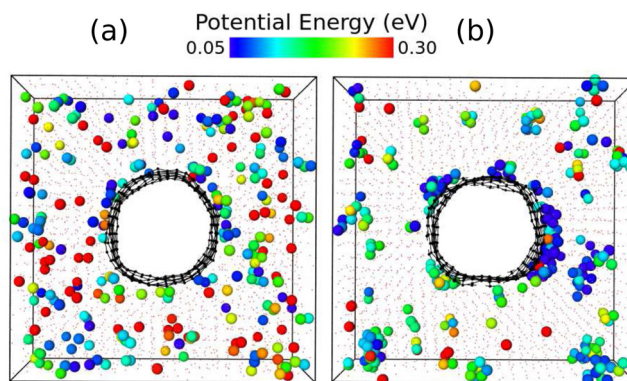


FIG. 2. MD snapshots: Ni are small red dots and C black spheres. He are the larger spheres and are colored according to their potential energy. The view is alongside the z -axis. (a) Initial configuration. (b) After 0.5 ns of simulation at 1000 K.

and occupy C vacancies, healing the CNT and allowing charge transfer to the nearest neighbor C atoms.

In order to mimic the situation of a localized region, where He is implanted by irradiation, we model a thin He layer (1 nm in thickness) and check the He diffusion into the matrix and into the CNT. In this case we three-fold replicate, along the z -axis, the $3.6\text{ nm} \times 3.6\text{ nm} \times 2.1\text{ nm}$ box mentioned above, and we simulate two cases. In the first one Ni atoms are replaced by He. In the second one we include defects in the CNT wall, i.e., we replace 10% of C/Ni atoms in the implanted layer by He, as shown in Fig. 3. The time evolution shows He bubble formation within the initial layer, plus He migration alongside the CNT wall. Within the simulation time only one He atom moved well outside the initial layer, and far from the CNT, while a large He bubble is nucleated directly on the CNT wall.

Using this potential, we calculate the mean square displacement of He interstitials in an Ni matrix and find an activation energy of around 0.75 eV. This value falls in between the classical result by Baskes and Melius,²² who found a barrier of 0.94 eV, and the *ab-initio* results by Xia *et al.*,²³ who obtained 0.48 eV. Experimental results¹⁰ vary between 0.5 eV and 2.5 eV. Also, we have calculated the diffusivity of He atoms alongside the CNT wall, which is many times faster than in the bulk. In addition to migration alongside the

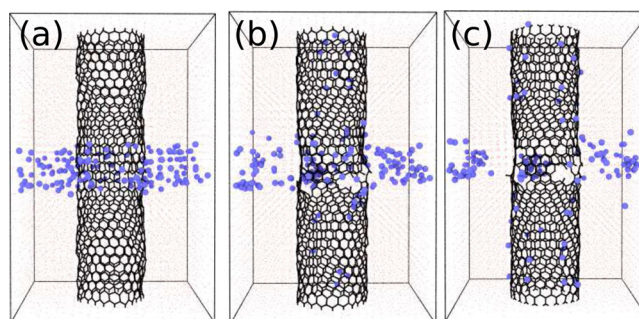


FIG. 3. MD simulation snapshots. Ni (small red dots), C (small black spheres), and He (blue spheres). (a) At $t=0$, when Ni/C atoms are replaced at random by He; (b) evolution 0.05 ns later; and (c) 1.0 ns later. In (b) and (c) He atoms are diffusing along the interior and exterior walls of the CNT, far from the CNT center. When no CNT wall defects are included He atoms diffuse only along the CNT external wall.

CNT wall, tens of He atoms diffuse rapidly into the CNT. However, the migration rate into the CNT decreases significantly due to Ni atoms occupying most CNT vacancy sites. However, those replacement Ni atoms deform the hexagonal lattice, and allow for a slow He penetration (i.e., of a few He atoms per ns). Helium then moves alongside the CNT, and could be easily outgassed by percolating CNT mats.²⁴ In the [supplementary material](#) a side and top view of such these events are shown.

We notice that the migration of He inside the CNT might lead to a feedback effect, since this would allow the continuous creation of free volume close to the CNT, which in turn would attract more He and enlarge the outgassing. Regarding other possible matrices like Al, a study on 1965 by Glyde and Mayne²⁵ indicated a barrier of about 1.5 eV. However, recent experiments²⁶ and *ab-initio* studies²⁷ seem to point to a barrier lower than 0.5 eV for He diffusion in Al, much lower than the Ni barrier. Therefore, He diffusion and clustering near CNTs inside an Al matrix would lead to faster He elimination, and higher radiation resistance, than in an Ni matrix.

We conclude that CNTs immersed in an Ni matrix can play the role of a He nano-chimney since He atoms can escape, and in this way reduce bubble formation inside the matrix. The interactions between absorbed gas, incoherent phase boundary, bubble morphology, and surface diffusion are generally complex, as revealed by recent *in situ* electron microscopy experiments.²⁸ For a CNT with defects, as expected when subject to radiation damage,²⁹ we have a transport mechanism distinct from grain boundaries or multi-layered materials: He atoms could diffuse into the CNTs and rapidly escape along the smooth walls. Therefore, composites made of CNTs inside metals may display enhanced radiation resistance, particularly relating to gas-induced swelling and embrittlement.

See [supplementary material](#) for an illustration of He trespassing a CNT wall.

We thank Aleksandar Staykov for valuable discussions. E.M.B. thanks support from PICT-0092 and a SeCTyP-UN Cuyo grant. This work was supported by the Fondo Nacional de Investigaciones Científicas y Tecnológicas (FONDECYT, Chile) under Grant Nos. 3140526 (R.G.), 1120399, and 1130272 (M.K.), and Financiamiento Basal para Centros Científicos y Tecnológicos de Excelencia FB-0807 (R.G., F.V., J.M., and M.K.). F.V. was supported by CONICYT

Doctoral Fellowship Grant No. 21140948. J.L. and K.P.S. acknowledge support by NSF DMR-1410636 and DMR-1120901.

- ¹M. Zhernenkov, S. Gill, V. Stanic, E. DiMasi, K. Kisslinger, J. K. Baldwin, A. Misra, M. J. Demkowicz, and L. Ecker, *Appl. Phys. Lett.* **104**, 241906 (2014).
- ²X.-M. Bai, A. Voter, R. Hoagland, M. Nastasi, and B. Uberuaga, *Science* **327**, 1631 (2010).
- ³E. M. Bringa, J. D. Monk, A. Caro, A. Misra, L. Zepeda-Ruiz, M. Duchaineau, F. Abraham, M. Nastasi, S. T. Picraux, Y. Q. Wang, and D. Farkas, *Nano Lett.* **12**, 3351 (2012).
- ⁴K. P. So, D. Chen, A. Kushima, M. Li, S. Kim, Y. Yang, Z. Wang, J. G. Park, Y. H. Lee, R. I. Gonzalez, M. Kiwi, E. M. Bringa, S. Lin, and J. Li, *Nano Energy* **22**, 319 (2016).
- ⁵K. P. So, X. Liu, H. Mori, A. Kushima, J. G. Park, H. S. Kim, S. Ogata, Y. H. Lee, and J. Li, "Ton-scale metal-carbon nanotube composite: The mechanism of strengthening while retaining tensile ductility," *Extreme Mech. Lett.* (published online).
- ⁶D. Bacon, Y. Osetsky, R. Stoller, and R. Voskoboynikov, *J. Nucl. Mater.* **323**, 152 (2003).
- ⁷I. Birss, *J. Nucl. Mater.* **34**, 241 (1970).
- ⁸V. Chernikov and P. Kazansky, *J. Nucl. Mater.* **172**, 155 (1990).
- ⁹E. Denisov, T. Kompaniets, A. Yukhimchuk, I. Boitsov, and I. Malkov, *Tech. Phys.* **58**, 779 (2013).
- ¹⁰P. Trocellier, S. Agarwal, and S. Miro, *J. Nucl. Mater.* **445**, 128 (2014).
- ¹¹S. Binyukova, I. Chernov, B. Kalin, A. Kalashnikov, and A. Timofeev, *Atom. Energy* **93**, 569 (2002).
- ¹²V. Chernikov, H. Trinkaus, and H. Ullmaier, *J. Nucl. Mater.* **250**, 103 (1997).
- ¹³X. Cao, Q. Xu, K. Sato, and T. Yoshiie, *J. Nucl. Mater.* **412**, 165 (2011).
- ¹⁴I. Beyerlein, A. Caro, M. Demkowicz, N. Mara, A. Misra, and B. Uberuaga, *Mater. Today* **16**, 443 (2013).
- ¹⁵S. J. Plimpton, *J. Comput. Phys.* **117**, 1 (1995).
- ¹⁶A. C. T. van Duin, S. Dasgupta, F. Lorant, and W. A. Goddard, *J. Phys. Chem. A* **105**, 9396 (2001).
- ¹⁷L. Meng, J. Jiang, J. Wang, and F. Ding, *J. Phys. Chem. C* **118**, 720 (2014).
- ¹⁸C. S. Spanjers, T. P. Senftle, A. C. T. van Duin, A. I. Frenkel, and R. M. Rioux, *Phys. Chem. Chem. Phys.* **16**, 26528 (2014).
- ¹⁹A. M. Kamat, A. C. T. van Duin, and A. Yakovlev, *J. Phys. Chem. A* **114**, 12561 (2010).
- ²⁰A. Stukowski, *Model. Simul. Mater. Sc.* **18**, 015012 (2010).
- ²¹J. Hetherly, E. Martinez, Z. Di, M. Nastasi, and A. Caro, *Scr. Mater.* **66**, 17 (2012).
- ²²M. I. Baskes and C. F. Melius, *Phys. Rev. B* **20**, 3197 (1979).
- ²³J. Xia, W. Hu, J. Yang, B. Ao, and X. Wang, *Phys. Status Solidi B* **243**, 579 (2006).
- ²⁴H. Verweij, M. C. Schillo, and J. Li, *Small* **3**, 1996 (2007).
- ²⁵H. R. Glyde and K. I. Mayne, *Philos. Mag.* **12**, 997 (1965).
- ²⁶B. Glam, D. Moreno, S. Eliezer, and D. Eliezer, *J. Nucl. Mater.* **393**, 230 (2009).
- ²⁷L. Yang, X. Zu, and F. Gao, *Physica B* **403**, 2719 (2008).
- ²⁸D.-G. Xie, Z.-J. Wang, J. Sun, J. Li, E. Ma, and Z.-W. Shan, *Nat. Mater.* **14**, 899 (2015).
- ²⁹O. Lehtinen, T. Nikitin, A. V. Krashennnikov, L. Sun, F. Banhart, L. Khriachtchev, and J. Keinonen, *New J. Phys.* **13**, 073004 (2011).